UCRL-CONF-226066

LAWRENCE
LIVERMORE
NATIONAL
LABORATORY

Crevice Repassivation Potentials for Alloy 22 in Simulated Concentrated Ground Waters

R. B. Rebak, K. J. Evans, G. O. Ilevbare

November 13, 2006

Corrosion/2007 Conference and Exposition
Nashville, TN, United States
March 11, 2007 through March 15, 2007

Disclaimer

This document was prepared as an account of work sponsored by an agency of the United States Government. Neither the United States Government nor the University of California nor any of their employees, makes any warranty, express or implied, or assumes any legal liability or responsibility for the accuracy, completeness, or usefulness of any information, apparatus, product, or process disclosed, or represents that its use would not infringe privately owned rights. Reference herein to any specific commercial product, process, or service by trade name, trademark, manufacturer, or otherwise, does not necessarily constitute or imply its endorsement, recommendation, or favoring by the United States Government or the University of California. The views and opinions of authors expressed herein do not necessarily state or reflect those of the United States Government or the University of California, and shall not be used for advertising or product endorsement purposes.

Paper 07584 prepared to be presented at CORROSION/2007 Conference and Exposition 11-15 March 2007 in Nashville, TN

CREVICE REPASSIVATION POTENTIALS OF ALLOY 22 IN SIMULATED CONCENTRATED GROUND WATERS

Raul B. Rebak, Kenneth J. Evans and Gabriel O. Ilevbare
Lawrence Livermore National Laboratory
7000 East Ave, L-631
Livermore, CA 94550, USA

ABSTRACT

The resistance of Alloy 22 (N06022) to localized corrosion, mainly crevice corrosion, has been extensively investigated in the last few years. However, the behavior of Alloy 22 in concentrated aqueous solutions that may simulate concentrated ground waters was not fully understood. Systematic electrochemical tests using cyclic potentiodynamic polarization as well as the Tsujikawa-Hisamatsu electrochemical method were performed to determine the crevice corrosion susceptibility of Alloy 22 in simulated concentrated water (SCW), simulated acidified water (SAW) and basic saturated water (BSW). Results show that Alloy 22 is immune to crevice corrosion in SCW and SAW but may suffer crevice corrosion initiation in BSW. Results also show that in a naturally aerated environment, the corrosion potential would never reach the critical potential for crevice corrosion initiation.

Keywords: N06022, Simulated Concentrated Water, Simulated Acidified Water, Simulated Basic Water, Temperature, Crevice Corrosion

INTRODUCTION

Alloy 22 (N06022) is nickel (Ni) based and contains nominally 22% Chromium (Cr), 13% Molybdenum (Mo) and 3% tungsten (W). [1] Alloy 22 belongs to the Ni-Cr-Mo family of nickel based alloys, which also include alloys such as C-4 (N06455), C-276 (N10276), C-2000 (N06200), 59 (N06059) and 686 (N06686). [1] The Ni-Cr-Mo alloys were designed to withstand the most aggressive industrial applications, including reducing acids such as hydrochloric and oxidizing acids such as nitric. Chromium is the beneficial alloying element added for protection against oxidizing conditions and molybdenum is the beneficial alloying element to protect against reducing conditions. [2-4] The base element (nickel) protects the alloy against caustic conditions. [2-4] All three elements, Ni, Cr and Mo act synergistically to provide resistance to environmentally assisted cracking in hot concentrated chloride solutions. [2-4] The alloying elements Cr and Mo also provide resistance to localized corrosion such as pitting and crevice corrosion

in chloride containing solutions. Some of the Ni-Cr-Mo alloys also contain a small amount of tungsten (W), which may act in a similar way as Mo regarding protection against localized corrosion. [5] Ni-Cr-Mo alloys are practically immune to pitting corrosion but they may suffer crevice corrosion under aggressive environmental conditions under the effect of chloride. The presence of other anions in the electrolyte inhibits crevice corrosion. [6-16] These anions include mainly nitrate, sulfate and carbonate. [6-16] A minimum ratio of inhibitor to chloride is needed for the inhibition to occur. [6-16] For example, for nitrate, it is generally accepted that a ratio (R) of concentration nitrate over concentration of chloride of 0.5 may be sufficient to inhibit crevice corrosion initiation and propagation in Alloy 22. [7,9,10,17]

Due to its excellent resistance to all forms of corrosion, Alloy 22 (N06022) has been selected to fabricate the external shell of the Yucca Mountain high-level nuclear waste containers. [18] The environment at the repository site is mostly dry or unsaturated. If water enters in contact with the containers it would be in the form of two main modes: (1) Dripping from the drift crown and walls and (2) Deliquescence of salts or dust collected during the early dry period. The dripping from the drift crown/wall is basically ground water and the main process by which it will enter in contact with the container is generally called seepage. Evaporation may cause these ground waters to concentrate on the engineered barriers. The enrichment of dilute ground waters will follow the chemical divide, that is, the nature and amount of each species that could be present in the final drop of water will depend on the relative amount of species in the originating water. [18] In general, during evaporation of seepage water a high concentration of nitrate develops, owing to the high solubility of nitrates. This is significant with respect to corrosion performance because the nitrate has inhibiting effects on localized corrosion initiation and propagation, as mentioned above. [6-16]

The objective of this paper was to examine the anodic behavior of Alloy 22 in waters that may simulate the conditions of concentrated ground waters. Electrochemical tests were performed in three different electrolyte solutions: (a) Simulated Concentrated Water (SCW), (b) Simulated Acidified Water (SAW) and (c) Basic Saturated Water (BSW) (Table 1).

EXPERIMENTAL

The specimens were machined from 1.25-inch thick plates (~32 mm). Table 2 shows the chemical composition of the material. The specimens were in the form of multiple crevice assemblies (MCA) or lollipops (Figure 1). The dimensions of the MCA were approximately 2 mm thick and a minimum of 11 cm long. The test part of the specimen was an annulus of 20 mm outside diameter and 7 mm inside diameter. For the electrochemical testing the MCA specimens were partially immersed, that is, water line crossed the stem of the specimen (Figure 1). The exposed surface area of each specimen depended on the immersion length of the specimens and was either 7.43 cm² or 10.68 cm². The area covered by the crevice formers was approximately 1.5 cm². The crevice formers (CF) were mounted on both sides of the specimen (Figure 1). Each crevice former consisted of a washer made of a ceramic material (alumina) containing 12 crevicing spots or teeth with gaps in between the teeth (ASTM G 48). [19] Before mounting them onto the metallic specimens, the CF were covered with PTFE tape to ensure a tight crevicing gap. The specimens had different types of surface finish (See Tables 3-6) for description of the surface finish. There are two types of specimens mentioned in this work: (1) The as-received wrought mill annealed (MA) or non welded and (2) The welded specimens, which included two subtypes: (2.a) The as-welded (ASW) and (2.b) the welded plus high-temperature aged (HTA). Thermal aging was carried out at 700°C for 173 hours, which would have produced second phase precipitation in the specimens. [20]

Table 1 shows the composition of the three test solutions. SCW is simulated concentrated water and it is approximately 1000 times more concentrated than ground water (pH may vary from 8 to 10), SAW is simulated acidified water and it is 1000 times more concentrated than ground water later acidi-

fied to pH 2.8, BSW is basic saturated water and it has a high pH of 13. Nitrogen (N_2) was purged through the solution at a flow rate of 100cc/min for 24 hours while the corrosion potential (E_{corr}) was monitored. Nitrogen bubbling was continued throughout all the electrochemical tests. The electrochemical tests were conducted in a one-liter, three-electrode, borosilicate glass flask (ASTM G 5). [19] A water-cooled condenser combined with a water trap was used to avoid evaporation of the solution and to prevent the ingress of air (oxygen). The tested temperatures were 60°C, 90°C, 100°C and 105°C. The temperature of the solution was controlled using a heating mantle or thermostatisized bath connected to a temperature control device. All the tests were carried out at ambient pressure. The reference electrode was saturated silver chloride (SSC) electrode, which has a potential of 199 mV more positive than the standard hydrogen electrode (SHE). The reference electrode was connected to the solution through a water-jacketed Luggin probe so that the electrode was maintained at near ambient temperature. The counter electrode was a large area flag of platinum foil spot-welded to a platinum wire. All the potentials in this paper are reported in the SSC scale.

Basically the test sequence for each specimen consisted of two parts: (1) E_{corr} evolution as a function of time for 24 h and (2) Cyclic Potentiodynamic Polarization (CPP) (ASTM G 61) [19] or Tsujikawa-Hisamatsu Electrochemical (THE) test. The CPP is one of the tests commonly used to assess the susceptibility of Alloy 22 to localized corrosion and its passive stability. The potential scan was started generally 150 mV below E_{corr} usually at a set scan rate of 0.167 mV/s. The scan direction was generally reversed when the current density reached 5 mA/cm^2 in the forward scan. Depending on the range of applied potentials, each CPP test could last between 1 h and 3 h. In the THE test the potential scan was started 150 mV below E_{corr} at a set potentiodynamic scan rate of 0.167 mV/s. Once the current density reached a predetermined value (for example 20 μA/cm² or 2 μA/cm²), the controlling mode was switched from potentiodynamic to galvanostatic and the predetermined current density is applied for usually 2 h. The resulting potential at the end of the galvanostatic treatment was recorded. After the galvanostatic step, the treatment was switched to a potentiostatic mode. The potentiostatic steps were applied for 2 h starting at the potential recorded at the end of the galvanostatic treatment and applying as many steps as necessary until crevice repassivation was achieved. Each subsequent potentiostatic step was 10 mV lower than the previous step. Generally 10 steps (or a total of 100 mV) were necessary to achieve repassivation of an active crevice-corrosion. The repassivation potential is determined as the potential for which the current density decreases as a function of time in the period of treatment of 2 h. Depending of the applied time and number of potentiostatic steps, each THE test could last up to 30 h.

After the CPP and THE tests, the specimens were examined in an optical stereomicroscope at a magnification of 20 times to establish the mode and location of the attack. A few specimens were also studied using a scanning electron microscope (SEM).

RESULTS AND DISCUSSION

The Corrosion Potential (E_{corr})

Tables 3-6 show the values of the corrosion potential (E_{corr}) for Alloy 22 specimens after 24-h immersion in the three deaerated electrolytes. The values of E_{corr} in Tables 3-6 are for comparative purposes only and they do not represent steady state values. That is, the values of E_{corr} in Tables 3-6 are not the values at which Alloy 22 would ultimately adopt when exposed to similar environments in aerated conditions for exposure times longer than 24-h.

Figure 2 shows the 24-h corrosion potential (E_{corr}) (open symbols) for Alloy 22 in the three deaerated electrolytes as a function of their ambient temperature pH values (Table 1). The 24-h E_{corr} values are the end values at 24 h. The average E_{corr} values shown in Figure 2 are for all the tested conditions in Table 3-6 including MA, ASW and ASW + HTA specimens also including more than one type

of surface finish. For SAW and SCW the E_{corr} values are for 60, 90 and 100°C and for BSW for 90 and 105°C. Figure 2 shows that as the pH increased the 24-h E_{corr} decreased. The largest standard deviations were for the alkaline solutions. The E_{corr} in the acidic solution was more reproducible. Figure 2 also shows the E_{corr} for Alloy 22 after long-term exposure in aerated electrolytes (full symbol) in the temperature range 60-105°C. [21-22] The exposure time for the aerated conditions varied from approximately 200 days to 1000 days. [22] It is evident that for the long-term aerated conditions the E_{corr} for all three electrolyte solutions is higher than for the short-term deaerated conditions. The raise of the E_{corr} for the longer immersion times suggests that the alloy becomes more passive in time by the development of a protective oxide film on the surface. This is especially prominent for the acidic solution for which the E_{corr} increased approximately 600 mV after a long term immersion in the aerated electrolyte likely via the development of a chromium oxide film on the surface. In the alkaline solutions (SCW and BSW) the long-term E_{corr} was approximately 250-300 mV higher than for the short term immersion in the deaerated solutions. Also, the standard deviation in the alkaline electrolytes was larger than in the acidic electrolyte. Again, as in the short term tests, E_{corr} decreased as the pH of the electrolyte increased.

Cyclic Potentiodynamic Polarizations (CPP)

Figure 3 shows the cyclic potentiodynamic polarization curves for Alloy 22 in deaerated SCW solution at 60°C and 90°C. The general behavior of Alloy 22 is practically the same at both temperatures. Both curves show an anodic peak in the middle of the passive region. At 90°C the anodic peak occurs at lower potentials than at 60°C. The existence of this anodic peak has been reported many times before. The occurrence of the anodic peak is pH and temperature dependent and it was shown that it occurs only when bicarbonate (HCO_3^-) is present in the electrolyte. [23] SCW is rich in bicarbonate ions (Table 1). At 90°C the passive current density and the breakdown potentials are slightly lower than at 60°C.

Figure 4 shows the polarization curves for as-welded (ASW) and welded plus high temperature aged (HTA) Alloy 22 in SCW at 90°C. Even though the HTA specimen should have a second phase of precipitated topologically closed packet (TCP) material [20] Figure 4 shows that both ASW and HTA materials behaved practically the same. Table 3 shows that none of the specimens tested in SCW at either 60 or 90°C suffered crevice corrosion after the CPP tests in spite of the high anodic applied potentials of approximately 1 V (Figures 3 and 4).

Figure 5 shows the cyclic potentiodynamic polarization curves for Alloy 22 in deaerated SAW solution at 60°C and 90°C. The general behavior of Alloy 22 is practically the same at both temperatures. Both curves show a large passive region between -100 mV and +700 mV SSC. The breakdown potential is slightly lower at 90°C. Similar passive behavior of Alloy in SAW solutions have been reported before. [24-25] Figure 6 shows the polarization curves for as-welded (ASW) and welded plus high temperature aged (HTA) Alloy 22 in SAW at 90°C. Even though the HTA specimen should have a second phase of precipitated topologically closed packet (TCP) material [20] Figure 6 shows that both ASW and HTA materials behave practically the same. Table 4 shows that none of the specimens tested in SAW at either 60 or 90°C suffered crevice corrosion after the CPP tests in spite of the high anodic applied potentials of more than 1 V (Figures 5 and 6).

Figure 7 shows the CPP curves for ASW Alloy 22 in BSW solution at 105°C at two different potential scan rates. Alloy 22 does not show the typical anodic peak in the region of passive potentials as the alloy exhibits in SCW solutions (Figures 3 and 4). Even though BSW has carbonate in its composition (Table 1), the pH of 13 is much higher than the pH required for stable presence of bicarbonate ions. Bicarbonate ions may exist at pH between 8 and 10, which is the pH of SCW solutions (Table 1). Both curves in Figure 7 have a similar shape, except that for the lower scan rate curve, the passive current density is lower. A lower potential scan rate allows the alloy to grow a more protective passive film and therefore producing a lower current output. Table 5 shows that after the test, the specimen scanned at

0.167 mV/sec was free from crevice corrosion (Figure 8) while the specimen scanned at a 10 times lower potential scan rate showed a slight amount of crevice corrosion (Figure 9). The only difference between the two tests (Table 5 and Figure 7) was time. For the slower scanned specimen the exposure time to high anodic potentials was ten times longer (e.g. 30 h vs. 3 h) therefore allowing time for crevice corrosion initiation.

Parameters from the Anodic Polarization Curves

In a cyclic potentiodynamic polarization (CPP) curves (e.g. Figures 3-7) there are several typical potentials. They can be divided in two groups: (1) Breakdown potentials in the forward scan, called E20 and E200 that represent the potential that needs to be applied to the specimen in the forward scan for the current density to reach respectively 20 μA/cm² and 200 μA/cm². (2) Repassivation potentials in the reverse scan, called ER10, ER1 and ERCO. ER10 and ER1 represent the potential that needs to be applied in the reverse scan for the current density to reach 10 μA/cm² and 1 μA/cm², respectively. ERCO represents the potential at which the reverse scan crosses over (CO) the forward scan in the passive region of potentials. [10] That is, in the forward scan, when the current density reaches for example 200 μA/cm² it can be considered that the alloy has lost its passive mode and that when the current density in the reverse scan has reached 10 or 1 μA/cm², the alloy has regained its passive behavior prior to the breakdown. Tables 3-5 list these parameters for Alloy 22 in SCW, SAW and BSW solutions, respectively.

CPP curves (Figures 4 and 6) showed little or no difference between the anodic behavior of ASW and ASW + HTA specimens. For example in SCW solution at 60°C, the average value of the breakdown potential E200 for MA and ASW specimens is 770 ± 19 mV SSC while the average E200 for ASW + HTA specimens is 773 ± 14 mV SSC (Table 3). These values are the same. Similarly, the repassivation potential ERCO for MA and ASW specimens is 635 mV ± 15 mV SSC and for the ASW + HTA specimens is 639 ± 17 mV SSC (Table 3). Because of the similarity on the breakdown and repassivation potentials between the MA or ASW and the ASW + HTA, in the following analyses, the parameters from the polarization curves for all types of metallurgical conditions will be grouped into one.

Figure 10 shows the breakdown potential E200 and the repassivation potential ERCO for all the tested Alloy 22 specimens in SCW (Table 3) as a function of the test temperature. Figure 11 is similar to Figure 10 but in the SAW solution. Again, for the acidic solution, the values of breakdown and repassivation potentials are higher than 600 mV SSC. The high values of breakdown and repassivation potentials for Alloy 22 in SCW and SAW (Figures 10 and 11) demonstrate that Alloy 22 is resistant to crevice corrosion in both electrolyte solutions.

The Tsujikawa-Hisamatsu Electrochemical (THE) Tests

Figure 12 shows a typical plot from a THE test. Both the potential and the current are plotted as a function of the test time. The potential at which the applied current does not increase as a function of time is the ER,CREV or crevice repassivation potential by the THE method. For Figure 12, the current does not increase as a function of time for the third potentiostatic step, that is, ER,CREV is 452 mV SSC. Table 6 shows the values of the repassivation potentials for ASW Alloy 22 using the THE method. Results show that Alloy 22 did not suffer crevice corrosion under the tested conditions in SCW and SAW solutions. Even though this method applies the current in a controlled manner over at least ten times longer time periods than the CPP tests, it was still impossible to nucleate crevice corrosion in Alloy 22 in these two electrolytes. Table 6 shows that it was possible to nucleate crevice corrosion in BSW solution both at 90°C and 105°C using the THE method. However, even though crevice corrosion was initiated in Alloy 22 in BSW solution, the repassivation potential was still higher than +400 mV SSC

(Table 6). Figure 13 shows the corroded appearance of specimen JE1618 with only minimal amount of crevice corrosion under the teeth of the crevice former.

Effect of Inhibitors

It was mentioned in the introduction that nitrate inhibits crevice corrosion initiation and propagation in Alloy 22. A minimum ratio (R) may be needed for this inhibition to occur. A generally accepted ratio R is in the order of 0.5. [8-10] However, this ratio R may depend on other variables such as total amount of chloride and temperature. [26] Table 1 shows that R is practically the same and approximately 1 for all the tested solutions in this paper (SCW, SAW and BSW). However, the total amount of chloride is much higher in BSW than in SAW and in SCW (in decreasing order). This may make BSW a more aggressive solution than SAW and SCW. Slow CPP and THE results show that the BSW electrolyte was able to initiate a small amount of crevice corrosion in Alloy 22 (Tables 5 and 6 and Figures 9 and 12) while both SCW and SAW could not initiate crevice corrosion in Alloy 22 (Tables 3 and 4).

Localized Corrosion Susceptibility in a Natural Environment

The model for localized corrosion stipulates that localized corrosion may occur in a natural aerated environment whenever the corrosion potential of the alloy in that environment (E_{corr}) reaches the critical value of repassivation potential (E_{crit}) measured under the same environmental conditions. [9] That is, if

$$\Delta E = E_{crit} - E_{corr} > 0 \qquad (1)$$

Crevice corrosion would not initiate. This relationship would also apply in the case pitting corrosion is the mode of attack for localized corrosion. Crevice corrosion may initiate only if E_{corr} is equal or higher than E_{crit}. The compliance of Equation 1 is a necessary but not sufficient condition. In many cases E_{corr} could be higher than E_{crit} but if the environment is not aggressive, crevice corrosion may not initiate. For example, if the environment has a large amount of inhibitive species (R>>1) crevice corrosion may not initiate even though the E_{corr} could reach high anodic values and be in the same order as E_{crit}. [27]

Figure 14 shows the long-term E_{corr} for Alloy 22 in aerated conditions (Figure 2) as a function of pH. Figure 14 also shows the breakdown potential E200 as well as the repassivation potential ERCO. Both E200 and ERCO could be ascribed as E_{crit} in Equation 1. Figure 14 clearly shows that in a naturally aerated environment the corrosion potential never reaches the critical potential for any of the tested multi-ionic electrolyte solutions. That is, under normal aeration conditions at temperature as high as 105°C, the value of ΔE is always positive. The smallest ΔE value in Figure 14 is for SAW solution and is in the order of 300 mV. SAW does not promote crevice corrosion in Alloy 22 (Tables 4 and 6). Both for SCW and BSW solution the value of ΔE is between 500 and 600 mV, which large margins for all practical purposes.

As a last remark, it is apparent that the current results show that aqueous electrolytes that simulate concentrated ground waters will not initiate crevice corrosion in Alloy 22, first because these electrolytes are rich in nitrate and second because the corrosion potential is always below a critical potential for crevice corrosion initiation.

CONCLUSIONS

1. The corrosion potential (E_{corr}) of Alloy 22 in concentrated aqueous solutions that may simulate concentrated ground waters is pH dependent. The higher the pH the lower the E_{corr}.

2. Alloy 22 is resistant to crevice corrosion initiation in simulated concentrated water (SCW) and simulated acidified water (SAW) up to 100°C.

3. The breakdown and repassivation potential of Alloy 22 in SCW and SAW it is the same for as-welded (ASW) and welded plus high temperature aged (HTA) materials.

4. Alloy 22 may be prone to crevice corrosion initiation in BSW at temperatures in the vicinity of 100°C

5. Alloy 22 may never suffer crevice corrosion under normal aeration conditions in all the three electrolytes (SCW, SAW and BSW) since the E_{corr} never reaches the critical potential for crevice corrosion initiation.

ACKNOWLEDGMENTS

This work was performed under the auspices of the U. S. Department of Energy (DOE) by the University of California Lawrence Livermore National Laboratory under contract N° W-7405-Eng-48. This work is supported by the Yucca Mountain Project, which is part of the Office of Civilian Radioactive Waste Management (OCRWM)

DISCLAIMER

This document was prepared as an account of work sponsored by an agency of the United States Government. Neither the United States Government nor the University of California nor any of their employees, makes any warranty, express or implied, or assumes any legal liability or responsibility for the accuracy, completeness, or usefulness of any information, apparatus, product, or process disclosed, or represents that its use would not infringe privately owned rights. Reference herein to any specific commercial product, process, or service by trade name, trademark, manufacturer, or otherwise, does not necessarily constitute or imply its endorsement, recommendation, or favoring by the United States Government or the University of California. The views and opinions of authors expressed herein do not necessarily state or reflect those of the United States Government or the University of California, and shall not be used for advertising or product endorsement purposes

REFERENCES

1. ASTM International, Annual Book of ASTM Standards, Volume 02.04 “Non-Ferrous Metals” Standard 575 B (West Conshohocken, PA: ASTM International, 2002)
2. R. B. Rebak and P. Crook, Transportation, Storage and Disposal of Radioactive Materials, PVP-Vol. 483, p. 131 (American Society of Mechanical Engineers, 2004: New York, NY)
3. R. B. Rebak in Corrosion and Environmental Degradation, Volume II, p. 69 (Wiley-VCH, 2000: Weinheim, Germany)

4. R. B. Rebak and P. Crook, *Advanced Materials and Processes*, February 2000
5. R. B. Rebak and P. Crook, Proceeding of the Symposium Critical Factors in Localized Corrosion III, PV 98-17, p. 289 (The Electrochemical Society, 1998: Pennington, NJ)
6. B. A. Kehler, G. O. Ilevbare and J. C. Scully, Corrosion, p. 1042 (2001)
7. G. A. Cragnolino, D. S. Dunn and Y.-M. Pan "Localized Corrosion Susceptibility of Alloy 22 as a Waste Package Container Material," Scientific Basis for Nuclear Waste Management XXV, Vol. 713, p. 53 (Materials Research Society 2002: Warrendale, PA)
8. D. S. Dunn, L. Yang, C. Wu and G. A. Cragnolino, Mat. Res. Soc. Symp. Proc. Vol 824 (MRS, 2004: Warrendale, PA)
9. J. H. Lee, T. Summers and R. B. Rebak, Paper 04692, Corrosion/2004 (NACE International, 2004: Houston, TX)
10. R. B. Rebak, Paper 05610, Corrosion/2005 (NACE International, 2005: Houston, TX)
11. R. M. Carranza, M. A. Rodríguez and R. B. Rebak, "Inhibition of Chloride Induced Crevice Corrosion in Alloy 22 by Fluoride Ions," Paper 06626, Corrosion/2006 (NACE International, 2006: Houston, TX)
12. G. O. Ilevbare, K. J. King, S. R. Gordon, H. A. Elayat, G. E. Gdowski and T. S. E. Summers, J. Electrochem. Soc., 152, 12, B547-B554, 2005.
13. D. S. Dunn, Y.-M. Pan, L. Yang and G. A. Cragnolino, Corrosion, 61, 1078 (2005).
14. D. S. Dunn, Y.-M. Pan, L. Yang and G. A. Cragnolino, Corrosion, 62, 3 (2006).
15. J. J. Gray, J. R. Hayes, G. E. Gdowski, and C. A. Orme, J. Electrochem. Soc., 153, B156-B161, 2006.
16. G. O. Ilevbare, Corrosion, 62, 340 (2006).
17. R. B. Rebak, "Mechanisms of Inhibition of Crevice Corrosion in Alloy 22," Fall 2006 MRS Meeting, Boston, MA 27Nov-01Dec06 (to be published).
18. G. M. Gordon, Corrosion, 58, 811 (2002).
19. ASTM International, Annual Book of ASTM Standards, Volume 03.02 "Wear and Erosion; Metal Corrosion" G-15, G-61, etc. (West Conshohocken, PA: ASTM International, 2004)
20. T. S. Edgecumbe Summers, T. Shen and R. B. Rebak "Prediction of the Lifetime Integrity of a Nuclear Waste Container Material Based on Thermal Stability Studies," International Conference on Ageing Studies and Lifetime Extension of Materials, St. Catherine's College, Oxford, UK July 12-14 1999, pp. 507-513 (Kluwer Academic / Plenum Publishers, 2001: New York, NY)
21. J. C. Estill, G. A. Hust and R. B. Rebak, "Long Term Corrosion Potential Behavior of Alloy 22 in Yucca Mountain Relevant Environments", Paper 03688 (Houston, TX: NACE International, 2003)
22. Unpublished Lawrence Livermore National Laboratory data
23. K.T. Chiang, D.S. Dunn, and G.A. Cragnolino, "The Combined Effect of Bicarbonate and Chloride Ions on the Stress Corrosion Cracking Susceptibility of Alloy 22," Paper 06506 (Houston TX: NACE International, 2006).
24. R. B. Rebak, T. S. Edgecumbe Summers, T. Lian, R. M. Carranza, J. R. Dillman, T. Corbin and P. Crook, "Effect of Thermal Aging on the Corrosion Behavior of Wrought and Welded Alloy 22," Paper 02542 (Houston TX: NACE International, 2002).
25. K. J. Evans and R. B. Rebak, "Passivity of Alloy 22 in Concentrated Electrolytes. Effect of Temperature and Solution Composition," PV2002-13, pp. 344-354 (The Electrochemical Society, 2002: Pennington, NJ).
26. R. B. Rebak, presentation to the Nuclear Waste Technical Review Board, 26 September 2006, Las Vegas, NV (www.nwtrb.gov/meetings/2006/sept/rebak.pdf).
27. M. A. Rodriguez, M. L. Stuart and R. B. Rebak, "Long Term Electrochemical Behavior of Creviced and Non-Creviced Alloy 22 in CaCl2 + Ca(NO3)2 Brines at 155°C," Paper 07577, Corrosion/2007 (NACE International, 2007: Houston, TX).

TABLE 1
CHEMICAL COMPOSITION OF THE TESTED SOLUTIONS (mg/L)

Ion	SCW pH 8-10	SAW pH 2.8	BSW pH 13
K^+	3400	3400	81,480
Na^+	40,900	40,900	231,225
Mg^{2+}	< 1	1000	---
Ca^{2+}	< 1	1000	---
F^-	1400	0	1616
Cl^-	6700	24,250	169,204
NO_3^-	6400	23,000	177,168
SO_4^{2-}	16,700	38,600	16,907
HCO_3^-/CO_3^{2-}	70,000	0	107,171
SiO_2 (aq.)	~ 40	~ 40	9038
$[NO_3^-]/[Cl^-]$	0.96	0.95	1.05
$[AOTC]/[Cl^-]$	14	2.5	1.8

AOTC = Anions other than chloride.

TABLE 2 -
CHEMICAL COMPOSITION IN WEIGHT % OF THE TESTED MCA SPECIMENS

Specimens/Element	**Ni**	**Cr**	**Mo**	**W**	**Fe**	**Others**
Nominal ASTM B 575	50-62	20-22.5	12.5-14.5	2.5-3.5	2-6	2.5Co-0.5Mn-0.35V (max)
Specimens DEA, Heat 2277-1-3265	~57	21.2	12.9	2.9	3.9	0.7Co-0.25Mn-0.17V
JE0001-JE0150, JE1601-JE1617 and JE1652-JE1670 Heat 059902LL1(Base)	59.56	20.38	13.82	2.64	2.85	0.17V-0.16Mn
JE0001-JE0150, , JE1601-JE1617 and JE1652-JE1670 Heat XX1753BG (Weld Wire)	59.70	20.54	14	3.10	2.08	0.2Mn-0.03V
JE1618-JE1651and JE1671-JE1700 Base Heat 059902LL1 (above) and Weld Wire Heat XX1829BG (right)	58.31	20.44	14.16	3.07	2.2	0.21Mn-0.15Cu-0.05V

TABLE 3
CHARACTERISTIC POTENTIALS FROM CYCLIC POTENTIODYNAMIC POLARIZATION CURVES FOR ALLOY 22 IN SIMULATED CONCENTRATED WATER (SCW), pH ~8

Specimen ID	Type of Specimen	T (°C)	$E_{corr,}$ 24 h (mV, SSC)	E20 (mV, SSC)	E200 (mV, SSC)	ER10 (mV, SSC)	ER1 (mV, SSC)	ERCO (mV, SSC)	Obser-vations After the Tests
JE0003	ASW MCA, AR	60	-268	286	757	615	611	642	No CC
JE0049	ASW MCA, AR	60	-414	300	775	608	315	651	No CC
JE0050	ASW MCA, AR	60	-388	325	804	377	346	641	No CC
JE0051	ASW MCA, AR	60	-406	302	775	340	314	648	No CC
DEA3210	MA MCA, AR	60	-404	299	764	597	595	624	No CC
DEA3211	MA MCA, AR	60	-413	315	790	631	628	656	No CC
DEA3212	MA MCA, AR	60	-401	299	763	348	309	609	No CC
DEA3213	MA MCA, AR	60	-411	302	771	342	303	625	No CC
DEA3214	MA MCA, AR	60	-412	299	765	599	282	635	No CC
DEA3215	MA MCA, AR	60	-284	270	733	610	270	623	No CC
JE0079	ASW + HTA MCA	60	-408	333	779	618	616	628	No CC
JE0080	ASW + HTA MCA	60	-259	336	782	347	311	630	No CC
JE0081	ASW + HTA MCA	60	-438	320	757	633	631	658	No CC
DEA1530	MA MCA, AR	90	-482	185	685	590	585	632	No CC
DEA1531	MA MCA, AR	90	-476	176	692	597	595	640	No CC
DEA1532	MA MCA, AR	90	-472	162	681	571	536	615	No CC
DEA1533	MA MCA, AR	90	-480	176	689	589	588	624	No CC
DEA3198	MA MCA, AR	90	-261	181	728	591	563	612	No CC
DEA3199	MA MCA, AR	90	-236	168	696	561	549	602	No CC
DEA3200	MA MCA, AR	90	-239	162	711	543	-137	593	No CC
DEA3201	MA MCA, AR	90	-168	179	694	569	532	590	No CC
DEA3202	MA MCA, AR	90	-312	158	714	555	-137	612	No CC
DEA3203	MA MCA, AR	90	-188	172	699	558	224	597	No CC
JE0004	ASW MCA, AR	90	-204	225	764	608	240	637	No CC
JE0052	ASW MCA, AR	90	-427	215	752	620	599	612	No CC
JE0053	ASW MCA, AR	90	-478	173	674	591	589	600	No CC
JE0054	ASW MCA, AR	90	-176	172	684	555	547	582	No CC
JE0082	ASW + HTA MCA	90	-426						
JE0083	ASW + HTA MCA	90	-506	190	595	555	550	643	No CC
JE0084	ASW + HTA MCA	90	-112	218	611	568	558	655	No CC
	AR = The surface condition is as received from manufacturer (may have EDM cut edges which rendered the edges more active). 600 = All surfaces of the specimen were freshly finished with paper 600 (I.e. 1-h prior to test). ASW = As-welded, MA = wrought mill annealed (non-welded). HTA = High Temperature Aged (173 h at 700°C). The specimens were aged AR and were not resurfaced after aging.								

TABLE 4
CHARACTERISTIC POTENTIALS FROM CYCLIC POTENTIODYNAMIC POLARIZATION CURVES FOR ALLOY 22 IN SIMULATED ACIDIFIED WATER (SAW), pH ~2.8

Specimen ID	Type of Specimen	T (°C)	$E_{corr,}$ 24 h (mV, SSC)	E20 (mV, SSC)	E200 (mV, SSC)	ER10 (mV, SSC)	ER1 (mV, SSC)	ERCO (mV, SSC)	Obser-vations After the Tests
JE0001	ASW MCA, AR	60	-271	717	773	710	644		No CC
JE0073	ASW + HTA MCA	60	-252	712	798	710	390	761	No CC
JE0074	ASW + HTA MCA	60	-218	720	786	631	317	731	No CC
JE0075	ASW + HTA MCA	60	-241	717	800	705	387	761	No CC
JE0055	ASW MCA, AR	60	-201	741	787	729	675	740	No CC
JE0056	ASW MCA, AR	60	-271	743	790	733	679		No CC
DEA3191	MA MCA, AR	90	-305	613	698	634	320		No CC
DEA3192	MA MCA, AR	90	-297	662	705	654	386		No CC
DEA3193	MA MCA, AR	90	-294		697	634	328		No CC
DEA3194	MA MCA, AR	90	-292	653	704	646	326		No CC
DEA3195	MA MCA, AR	90	-305	641	704	642	302		No CC
DEA3196	MA MCA, AR	90	-300	601	697	469	206		No CC
DEA3197	MA MCA, AR	90	-303	627	697	641	320		No CC
JE0002	ASW MCA, AR	90	-270	674	703	648	592	633	No CC
JE0047	ASW MCA, AR	90	-288	680	723	662	597	670	No CC
JE0048	ASW MCA, AR	90	-262	679	709	653	593	638	No CC
JE0076	ASW + HTA MCA	90	-259	664	728	645	337	669	No CC
JE0077	ASW + HTA MCA	90	-262	655	719	610	221	653	No CC
JE0078	ASW + HTA MCA	90	-274	646	721	647	278	714	No CC
AR = The surface condition is as received from manufacturer (may have EDM cut edges which rendered the edges more active). 600 = All surfaces of the specimen were freshly finished with paper 600 (I.e. 1-h prior to test). ASW = As-welded, MA = wrought mill annealed (non-welded). MCA = multiple crevice assembly or lollipop. HTA = High Temperature Aged (173 h at 700°C). The specimens were aged AR and were not resurfaced after aging. Blank spaces (for example under ERCO) means that the data does not exist (i.e. no cross-over).									

TABLE 5
CHARACTERISTIC POTENTIALS FROM CYCLIC POTENTIODYNAMIC POLARIZATION CURVES FOR ALLOY 22 IN BASIC SATURATED WATER (BSW), pH ~13

Specimen ID	Type of Specimen	T (°C)	$E_{corr,}$ 24 h (mV, SSC)	E20 (mV, SSC)	E200 (mV, SSC)	ER10 (mV, SSC)	ER1 (mV, SSC)	ERCO (mV, SSC)	Obser-vations After the Tests
JE1623	ASW MCA, 600	105	-381	478	564	455		464	No CC
JE1642	ASW MCA, 600	105	-286	521	591	470	412	430	CC
600 = All surfaces of the specimen were freshly finished with paper 600 (I.e. 1-h prior to test). ASW = As-welded, MCA = multiple crevice assembly or lollipop. Specimen JE1623 was scanned at 0.167 mV/s and specimen JE1642 at 0.0167 mV/s									

TABLE 6
CHARACTERISTIC POTENTIALS FROM THE TSUJIWAWA-HISAMATSU ELECTROCHEMICAL TESTS FOR ALLOY 22 MULTI-IONIC SOLUTIONS

Specimen ID	Type of Specimen	Electrolyte	T (°C)	$E_{corr,}$ 24 h (mV, SSC)	ER,CREV (mV, SSC)	Observa-tions After the Tests
JE1603	ASW MCA, 600	SCW	90	-162	626	No CC
JE1604	ASW MCA, 600	SCW	90	-175	637	No CC
JE1613	ASW MCA, 600	SCW	100	-242	541	No CC
JE1641	ASW MCA, 600	SCW	100	-201	103	No CC
JE1601	ASW MCA, 600	SAW	90	-222	661	No CC
JE1602	ASW MCA, 600	SAW	90	-230	660	No CC
JE1612	ASW MCA, 600	SAW	100	-294	639	No CC
JE1614	ASW MCA, 600	BSW	90	-405	488	CC
JE1611	ASW MCA, 600	BSW	105	-293	452	CC
JE1618	ASW MCA, 600	BSW	105	-628	421	CC
600 = All surfaces of the specimen were freshly finished with paper 600 (I.e. 1-h prior to test). ASW = As-welded, MCA = multiple crevice assembly or lollipop						

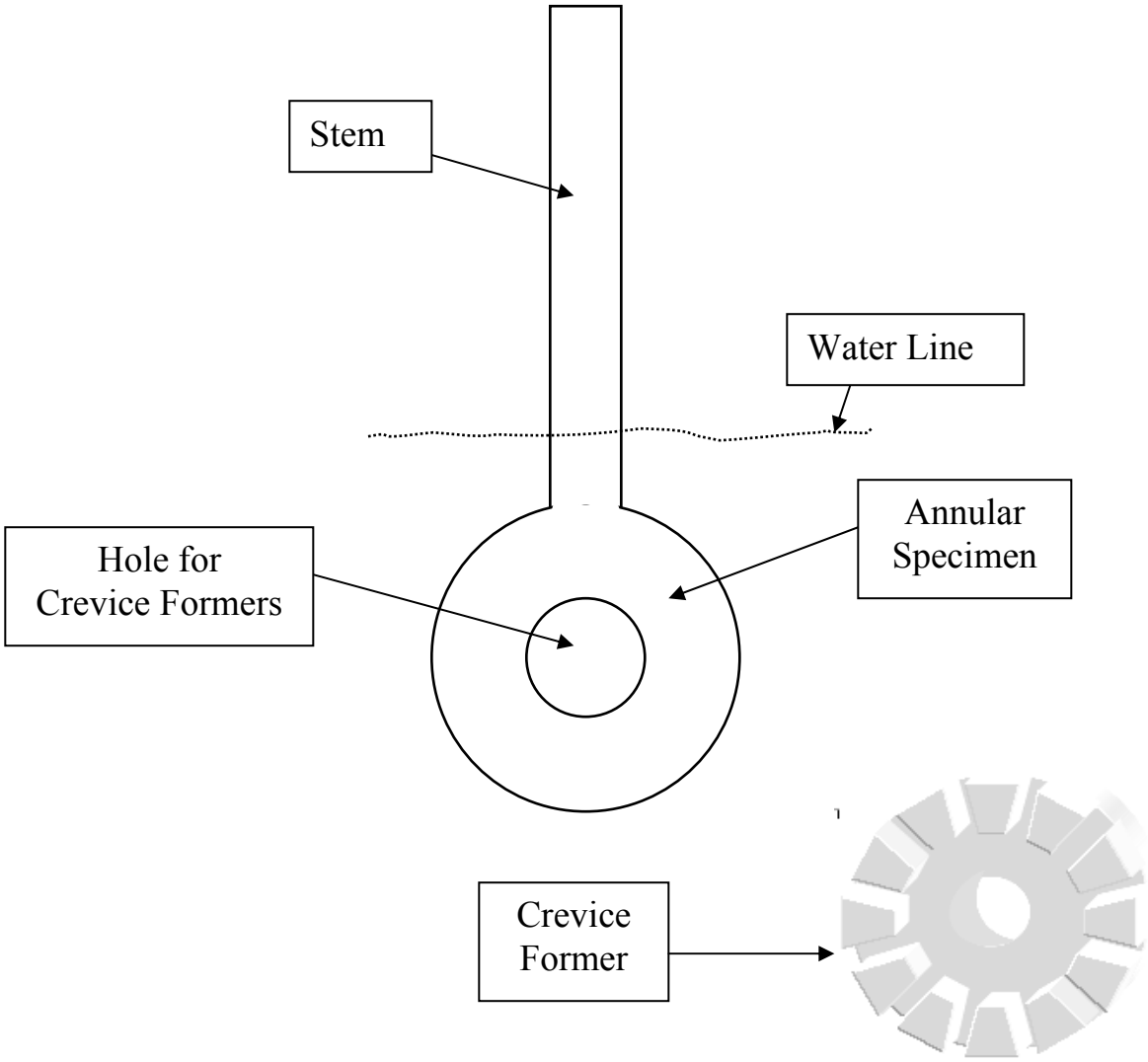

FIGURE 1 – Multiple Crevice Assembly (MCA) Specimen and Crevice Former (CF).

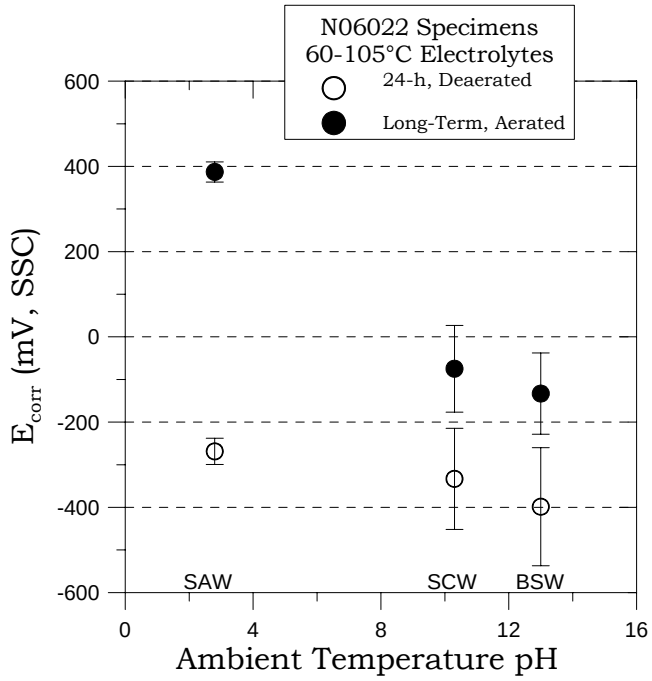

FIGURE 2 – Corrosion potential (E_{corr}) for Alloy 22 in multi-ionic electrolytes

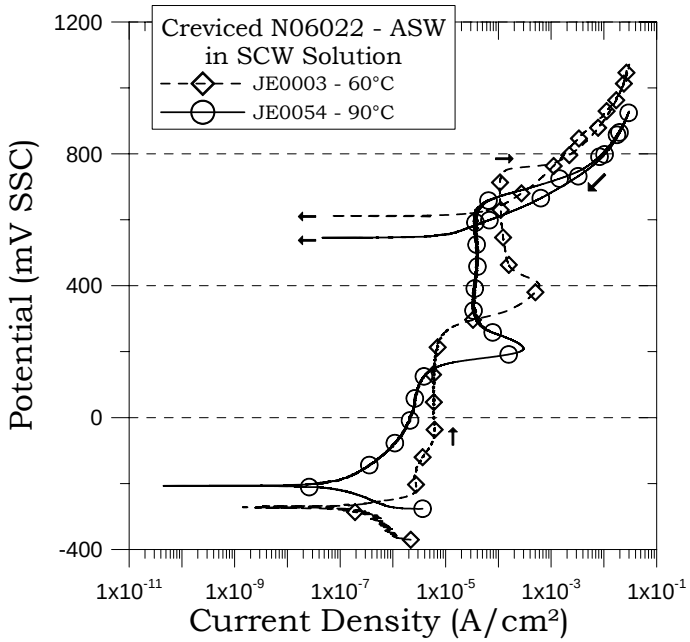

FIGURE 3 – Polarization curves for ASW Alloy 22 in SCW Solution at 60°C and 90°C

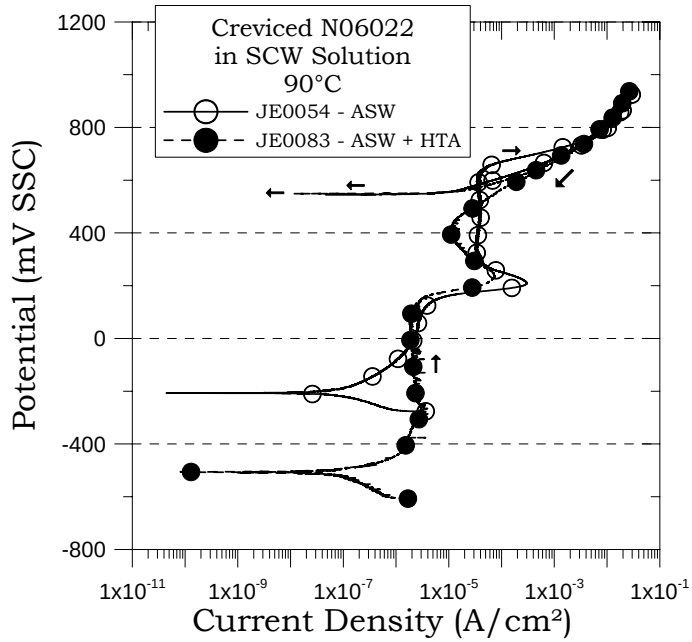

FIGURE 4 – Polarization curves for ASW and ASW + HTA Alloy 22 in SCW Solution at 90°C

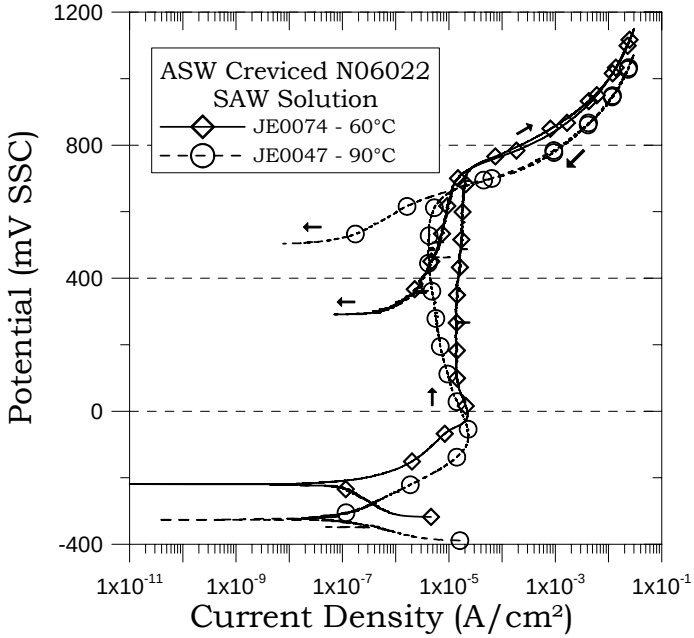

FIGURE 5 – Polarization curves for ASW Alloy 22 in SAW Solution at 60°C and 90°C

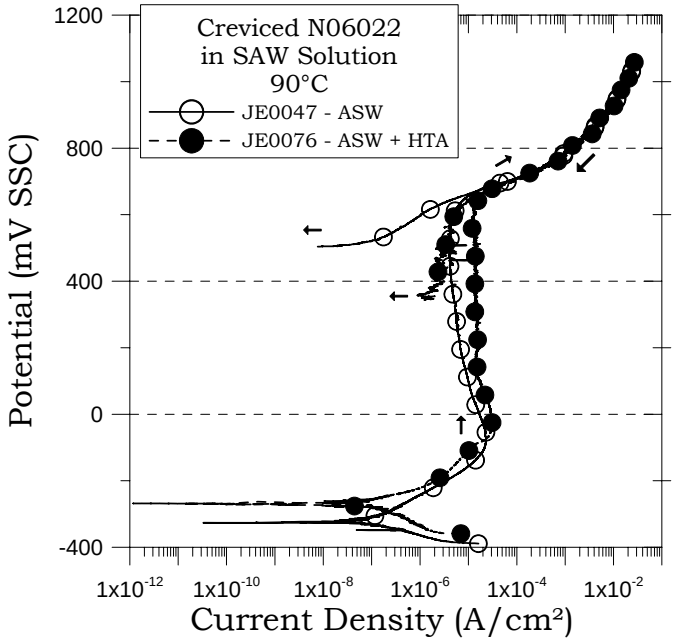

FIGURE 6 – Polarization curves for ASW and ASW + HTA Alloy 22 in SAW Solution at 90°C

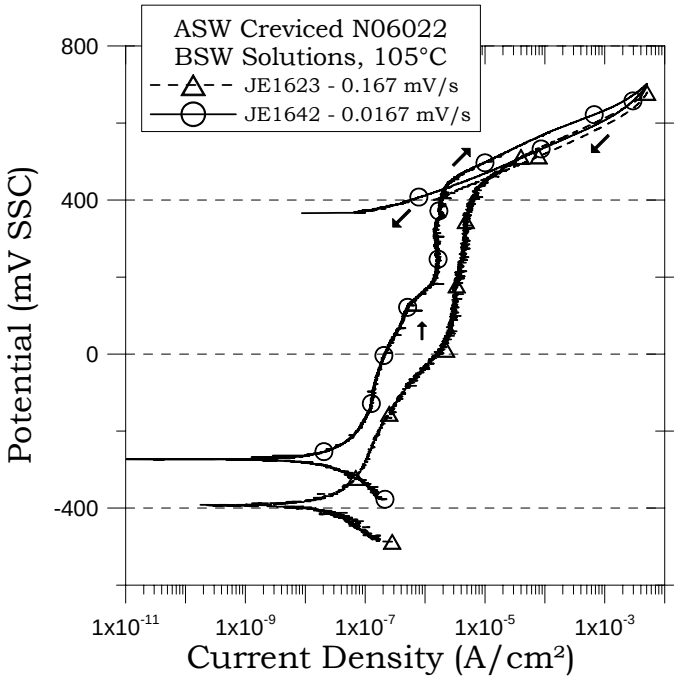

FIGURE 7 – Polarization curves for ASW Alloy 22 in BSW Solution at 105°C

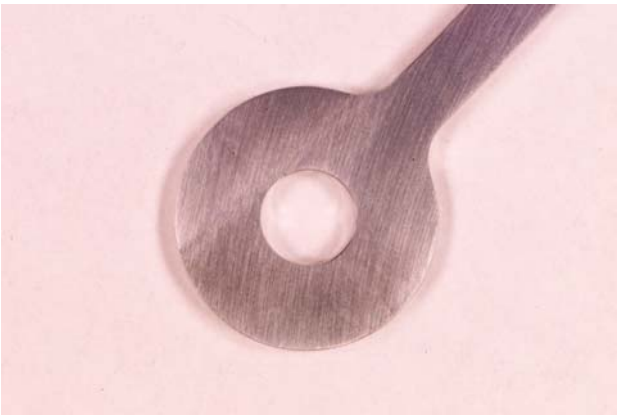

FIGURE 8 – Specimen JE1623 after CPP in BSW at 105°C. Scan Rate – 0.167 mV/s. No crevice corrosion

FIGURE 9 – Specimen JE1642 after CPP in BSW at 105°C. Scan Rate – 0.0167 mV/s. Small amount of crevice corrosion

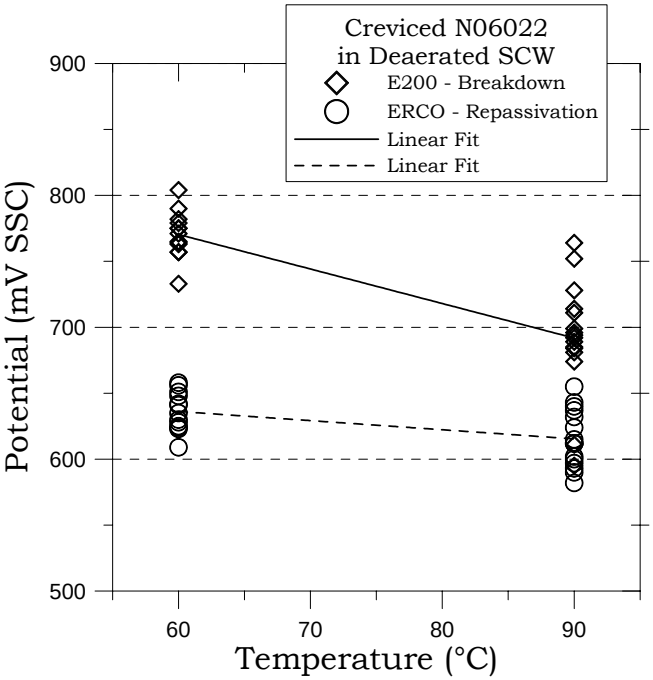

FIGURE 10 – Breakdown and repassivation potentials for Alloy 22 in SCW solution.
None of the specimens suffered crevice corrosion

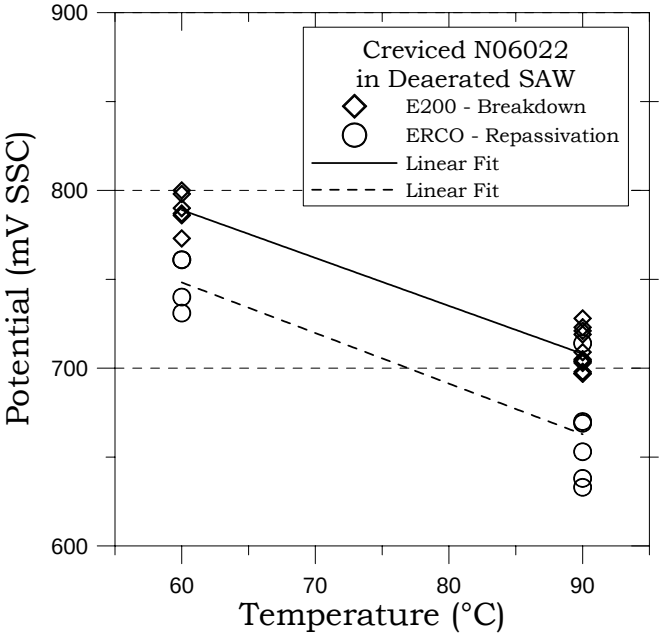

FIGURE 11 – Breakdown and repassivation potentials for Alloy 22 in SAW solution.
None of the specimens suffered crevice corrosion

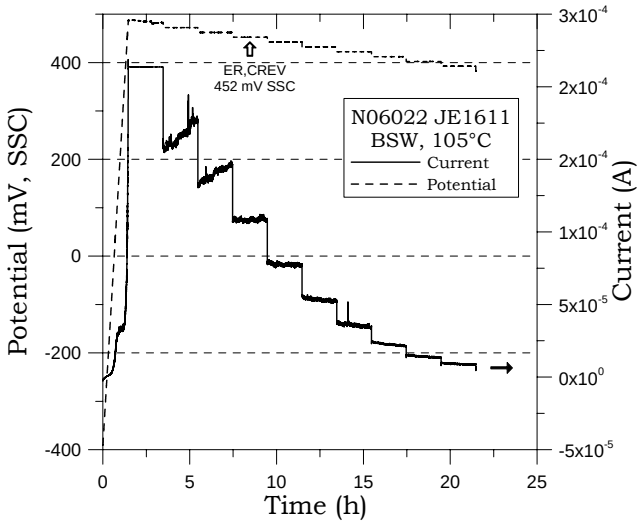

FIGURE 12 – Behavior of JE1611 using the THE method. Crevice corrosion occurred but the repassivation potential was high.

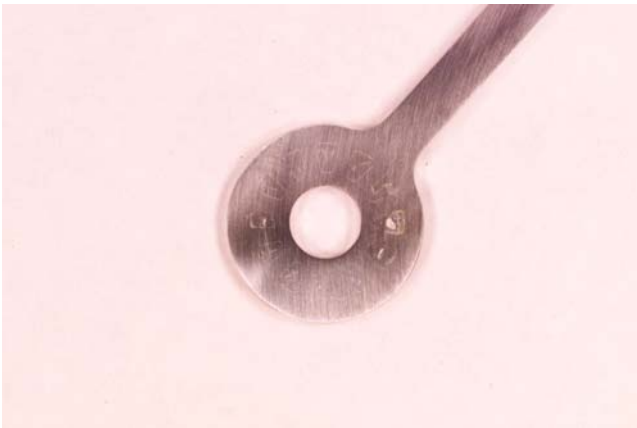

FIGURE 13 – Appearance of JE1618 after the THE test. Minimal amount of crevice corrosion can be seen under the crevice formers

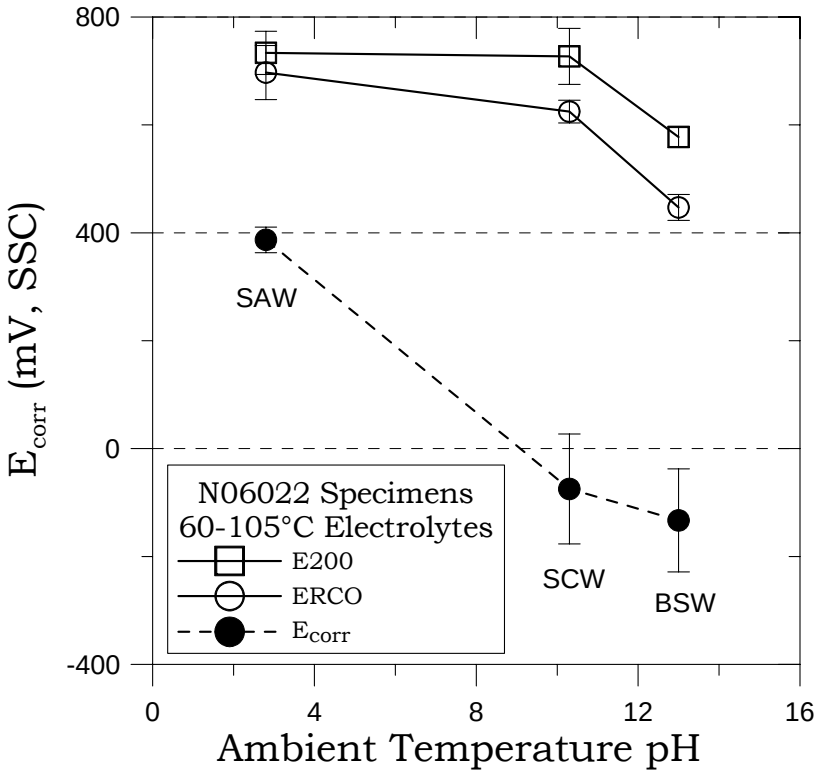

FIGURE 14 – E_{corr} and E_{crit} for Alloy 22 in the three tested electrolytes.